Synthesis, Oxidant Properties, and Antitumoral Effects of a Heteroleptic Palladium(II) Complex of Curcumin on Human Prostate Cancer Cells

Alessandra Valentini,*[,†] Franco Conforti,[†] Alessandra Crispini,[‡] Angelo De Martino,[§] Rossella Condello,[†] Chiara Stellitano,[†] Giuseppe Rotilio,[§] Mauro Ghedini,[‡] Giorgio Federici,[†] Sergio Bernardini,[†] and Daniela Pucci[‡]

Department of Laboratory Medicine, UOC Clinical Molecular Biology, PTV-Hospital University "Tor Vergata", Via Oxford 81, 00133 Rome, Italy, Centro di Eccellenza CEMIF, CAL-LASCAMM, Unità INSTM della Calabria, Department of Chemistry, Università della Calabria, Arcavacata di Rende (CS), Italy, Department of Biology, Università di Roma "Tor Vergata", Rome, Italy

Received October 8, 2008

A new ionic Pd(II) complex, [(bipy)Pd(Pcurc)][CF_3SO_3], **1**, with the metal center coordinated to two different chelating ligands, the pure curcumin (Pcurc) and the 4,4′-dinonyl-2,2′-bipyridine (bipy), has been synthesized, fully characterized, and its antitumoral mechanism and oxidant property have been investigated. The Pd(II) complex induces both cell growth inhibition and apoptosis of human prostate cancer cells, (LnCaP, PC3, and DU145) through the production of ROS and JNK phosphorylation associated with GSTp1 down-regulation. ROS production induced by complex **1** treatment activated apoptotis through mitochondrial membrane depolarization in all prostate cancer cells, with up-regulation of Bax and down-regulation of Bcl-2 proteins. In addition, while curcumin determines DNA damage and PARP cleavage, complex **1** does not elicit any activation of PARP enzyme. Taken together, these data validate the significance of curcumin complexation to a metal center and its conjugation to another functionalized bioactive ligand in the apoptosis signal transduction and enhancement of cell death in prostate cancer cell lines and suggest the potential of this design strategy in the improvement of the metal-based drugs cytotoxicity.

Introduction

Curcumin [1,7-bis(4-hydroxy-3-methoxyphenyl)-1,6-heptane-3,5-dione] is the major yellow pigment extracted from turmeric, the powdered rhizome of the perennial herb *Curcuma longa* L. Consumption of curcumin has been associated with a plethora of beneficial effects on human health, predominant among them are the anti-inflammatory and cancer chemopreventive activities.[1] Recently, the study of the mechanism of curcumin and its analogues in the chemopreventive activity has attracted increasing attention.[2,3] Curcumin exhibits remarkable cytotoxic effects on various cell lines and in particular down-regulates cell survival mechanisms in human prostate cancer cell lines.[4,5] Moreover, it has also been demonstrated that curcumin induces pro-apoptotic effects in several in vitro studies, mostly through the mitochondria-mediated pathway of apoptosis. Curcumin-mediated regulation of apoptosis involves caspases, Bcl-2 family members, inhibitors of apoptosis proteins, and heat shock proteins.[5,6] Furthermore, curcumin acts as free radical scavenger and antioxidant, inhibiting oxidative DNA damage and some Curcuminoid derivatives induce glutathione S-transferase, being potent inhibitor of cytochrome P450.[7] It has been observed that Curcumin-induced ROS[a] was suppressed by the addition of NAC, a precursor of GSH. GSH, in fact, important substrate for glutathione peroxidase and transferase, as well as scavenger of free radicals in cells. Oxidative modification of redox-sensitive factors and intermediate signaling molecules (i.e., JNK) are involved in ROS-mediated modulation of cell growth and cell survival characterized by the induction of apoptosis or necrosis.[8]

It has been observed that tetrahydroxycurcumin (1,7-bis(4-hydroxy-3-methoxyphenyl)heptane-3,5-dione) without the α, β-unsaturated carbonyl moiety does not produce intracellular ROS in HSG or HGF cells, even after visible light irradiation or HRP/H_2O_2 treatment.[9] These findings suggest that both the α, β-unsaturated carbonyl moiety of curcumin and the OH groups are responsible for intercellular ROS formation. Curcumin depletes hepatocyte GSH to a greater extent than can be explained by GSSG formation, presumably because GSH transferases catalyze GSH conjugate formation with the α,β-unsaturated carbonyl moiety of curcumin.[10]

Recently, we have reported the synthesis and the preliminary biological results of some new bifunctional complexes based on cyclopalladated 4-hexadecyloxycarboxylate-2-phenylquinoline and curcuminoid fragments. Treatment of DU145 human prostate cancer cells with these derivatives showed their effectiveness as antitumor agents with greater cytotoxicity than curcumin.[11]

These results encouraged us to continue further investigations on this subject following this promising synthetic strategy, and we decided to join, around the Pd(II) center, besides the curcumin, a bioactive chelating component, a 2,2′-bipyridine substituted in 4,4′ positions (bipy) with two aliphatic chains, instead of a cyclopalladating ligand. The presence of a *N,N* chelating ligand gives rise to a ionic complex, introducing electrostatic interactions and improving the cytotoxic properties of the resulting complex by increasing its solubility.

In the present study, we report the synthesis of a new ionic complex [(bipy)Pd(Pcurc)][CF_3SO_3], **1** (bipy = 4,4′-dinonyl-

* To whom correspondence should be addressed. Phone: +390620902259. Fax: +390620902357. E-mail: ales_valentini@yahoo.it.

† Department of Laboratory Medicine, UOC Clinical Molecular Biology, PTV-Hospital University "Tor Vergata".

‡ Centro di Eccellenza CEMIF, CAL-LASCAMM, Unità INSTM della Calabria, Department of Chemistry, Università della Calabria.

§ Department of Biology, Università di Roma "Tor Vergata".

[a] Abbreviations: ROS, reactive oxygen species; JNK, Jun N-terminal kinase; GSTp1, glutathione S-transferase pi; PARP, poly(ADP-ribose) polymerase; NAC, *N*-acetyl-L-cysteine; HSG, human submandibular gland; HGF, hepatocyte growth factor; HRP/H_2O_2, horseradish peroxidase/hydrogen peroxide; GSH, reduced glutathion; GSSG, glutathione disulfide; PGE, platinum group elements; HPLC, high performance liquid chromatography; GSTs, glutathione S-transferases; GS-X, glutathione conjugate; ΔΨmt, mitochondrial transmembrane potential; CCCP, carbonylcyanide *m*-chlorophenylhydrazone.

10.1021/jm801276a CCC: $40.75
Published on Web 12/29/2008

Scheme 1. Synthesis of [(bipy)Pd(Pcurc)][CF_3SO_3], complex **1**

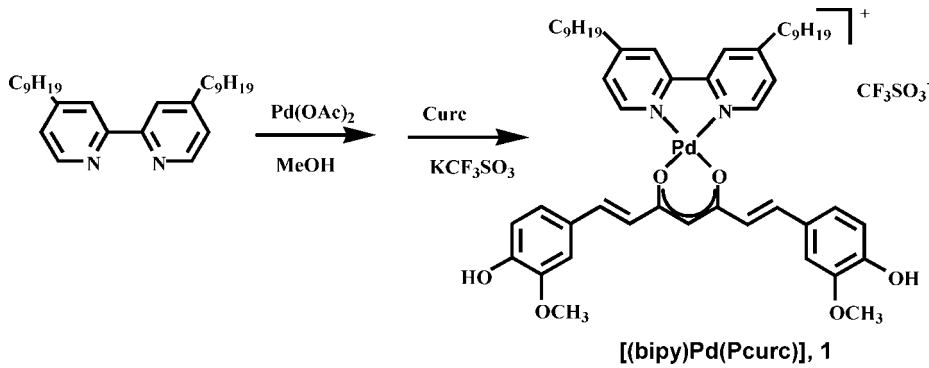

2,2′-bipyridine) curcumin carrier and the investigation of its activity in apoptosis induction and oxidant property on human prostate cancer cell lines. To understand the mechanism of action of complex **1**, we explore its ability in cell growth inhibition, ROS production, JNK activation, and cell death through mitochondrial bearing membrane depolarization.

Results and Discussion

Synthesis and Characterization of Complex 1. The synthesis of [(bipy)Pd(Pcurc)][CF_3SO_3], complex **1** was carried out starting from the 4,4′-dinonyl-2,2′-bipyridine (bipy) in two steps as shown in Scheme 1: (i) synthesis of the precursor [(bipy)Pd($OAc)_2$], performed stirring the ligand with palladium(II) acetate in a methanolic solution; (ii) reaction of [(bipy)Pd($OAc)_2$] with one equivalent of the previously purified curcumin and triflate potassium salt [KCF_3SO_3].

The isolated products have been fully characterized by IR, ^{1}H NMR, and elemental analysis, confirming the hypothetic stoichiometry. The presence in the IR spectra of the characteristic band of the triflate group at 1277 cm^{-1} has confirmed the ionic nature of complex **1**.

The behavior of complex **1** and of curcumin purified from other components,[11] namely pure-curcumin (pCurc) in physiological pH aqueous conditions has been investigated by UV/visible (UV/vis) spectroscopy over the time, in order to verify if photodegradation[12,13,14] phenomena, responsible for the limited use of curcumin in pharmaceutical applications, can be overcome through the substitution of the keto−enolic hydrogen atom with the palladated fragment. Indeed, complex **1** is very stable at physiological condition as proved by the absence of any shift in the position of the absorption maxima in the UV/vis spectrum over the time (Figure 1B), confirming that the presence of the mutual chelate rings prevents the degradation of the curcumin structure.

Cytotoxicity, Cell Growth Inhibition, and Induction of Apoptosis. We have investigated the effect of the new mononuclear ionic complex [(bipy)Pd(pCurc)][CF_3SO_3] **1** against human prostate cancer cell lines. We calculated the IC_{50} value of both complex **1** and its precursor pCurc, after 72 h of treatment of prostate cancer cells (LnCaP-SF, LnCaP, PC3, and DU145) by MTS assay (described in experimental section). As reported in the Table 1, we observed that complex **1** is less toxic than pCurc in all cell lines analyzed because the IC_{50} value range of 24−19.7 μM is significantly different from the one calculated for pCurc (2.2−7.8 μM). On the other hand, LnCaP-SF seems to be resistant to the toxic effects of both complex **1** and pCurc because the toxic effect was observed at the concentration higher than 100 μM. These preliminary data indicate that complex **1** is more active than Curc in inhibiting cell proliferation, suggesting both the purification of commercial curcumin and the global change in curcumin structure after complexation, is a winning strategy in order to enhance the cytotoxic activity of curcumin derivatives.[5] Therefore, to explain the proliferation inhibition due to pCurc and complex **1** treatment, we followed the growth of prostate cancer cells untreated (control) and treated with complex **1** or with pCurc at the correspondent IC_{50} values. Growth inhibition of prostate cancer cells treated with complex **1** is about 55% and stable during the growth curve, as shown in Figure 2. pCurc affected prostate cancer cells growth within no more than three days: on the fourth day, in fact, a rescue of DU145 cell growth is observed. Same data are obtained for the other prostate cancer cells studied. To investigate the biological effect of complex **1** on prostate cancer cells, we evaluated the induction of apoptosis and cell cycle perturbation by flow cytometry analysis. We observed that complex **1** was able to induce apoptosis in all cell lines analyzed except for LnCaP-SF cells (100 μM). At the IC_{50} value, complex **1** was able to induce 45% of apoptosis in LnCaP cells, 52% in PC3 cells, and 28% in DU145 cells, after 72 h of exposure. Moreover in all cell lines, pCurc induced G2 arrest after both 48 h (data not shown) and 72 h of exposure to the correspondent IC_{50} value, with only 12% of apoptosis induction after 72 h of treatment in LnCaP cells (Figure 3A). To verify the apoptosis induction due to complex **1** treatment, we analyzed the activation of caspase 3 and we observed that the enzyme is more active in complex **1** treated cells than in those treated with pCurc (Figure 3B). In addition, densitometric analysis of caspase 3 cleavage indicates that caspase is active in all prostate cancer cells analyzed and that in LnCaP-SF cells complex **1** and pCurc did not induce caspase 3 cleavage as expected. These data prove that the growth inhibition of prostate cancer cells treated with the Pd(II) complex **1** was determined by apoptosis induction, while pCurc simply delayed cell growth by inducing G2/M arrest.

ROS Production, GSH Depletion, and JNK Activation in Prostate Cancer Cells. It has been described recently that the role of ROS in curcumin-induced apoptosis is controversial[15] because curcumin can exert both pro- and antioxidant effects. Indeed, sensitivity of many tumor cells to curcumin is related to ROS generation and many well-known antioxidants prevent curcumin-induced apoptosis.[15−17] At the same time, curcumin is a potent scavenger of ROS and increases the level of glutathione.[18,19] ROS generation, due to oxidative stress, is determined by two opposite effects such as the production and the removal of free radicals, and it is at least in part responsible for toxic effects in drugs containing PGE. This mechanism is highly probable also for Pt(II) and Pt(IV). On the contrary, Pd(II)

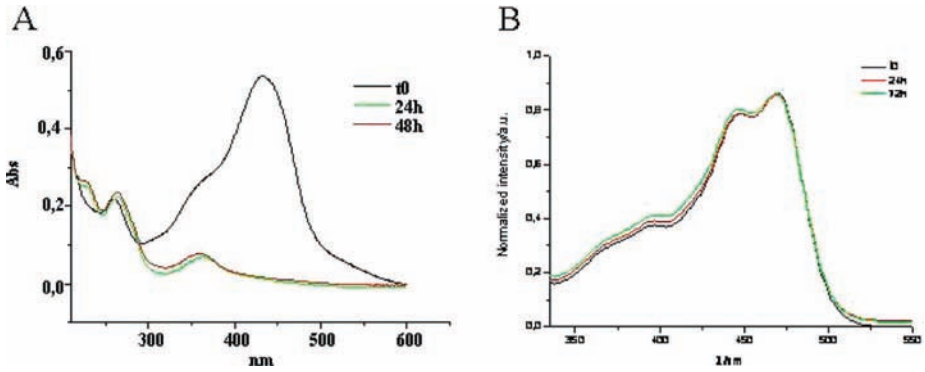

Figure 1. UV/vis evaluation for stability of complex **1**. UV/vis spectra of pCurc (A) and complex **1** (B) in EtOH solution at 7.2 pH after 24, 48, and 72 h.

Table 1. IC_{50} Value for pCurc and Complex **1** against Prostate Cancer Cell Lines

	$IC_{50} \pm SD$	
	pCurc (μM)	complex **1** (μM)
LnCaP-SF	>100	>100
LnCaP	7.8 ± 1.5	19.7 ± 1.1
PC3	2.0 ± 2.2	22.2 ± 0.5
DU145	2.25 ± 0.7	24.2 ± 1.1

and Cd(II) have no effect on ROS induction, although they show considerable toxicity.[20−22]

Hence, we investigated the ROS production in PC3 and DU145 cells treated with complex **1** and pCurc at the concentration to IC_{50} value, respectively. As shown in Figure 4A, pCurc at the 3 μM value was able to induce ROS production two times more than complex **1** at 25 μM value after 18 h of exposure in both PC3 and DU145 cells. These data indicate that complex **1** displays, in prostate cancer cells, lower oxidant properties than pCurc, maybe due to the fact that pCurc indirectly is able to determine the increases level of glutathione in response to ROS generation.[18,19]

It is known that curcumin depletes hepatocyte GSH to a greater extent that can be explained by GSSG formation, presumably because GSH transferases catalyze GSH conjugate formation with the α,β-unsaturated carbonyl moiety of curcumin.[10] However, the use of a modified structure for curcumin with the presence of a metal blocking its α,β-unsaturated carbonyl moiety allowed us to think of some different modulation of GSH and GSTp1 related protein. Figure 4B shows the analysis obtained by HPLC of GSH concentration in the case of DU145 cells treated with pCurc and complex **1**, respectively. The amount of GSH (expressed as nmol GSH/mg protein) is higher in pCurc treated cells than in complex **1** treated cells. This increase of GSH concentration is evaluated already after 12 h of treatment with pCurc and maintained up to 48 h of exposure, with a maximum after 24 h, suggesting that the reduction of GSH may be due to the formation of thiolic groups. Analogous data are observed for LnCaP and PC3 cells. Therefore, these data suggest that pCurc exhibits direct oxidant property and indirect antioxidant property, while complex **1** inducing a decrease in GSH amount exhibits only oxidant property.

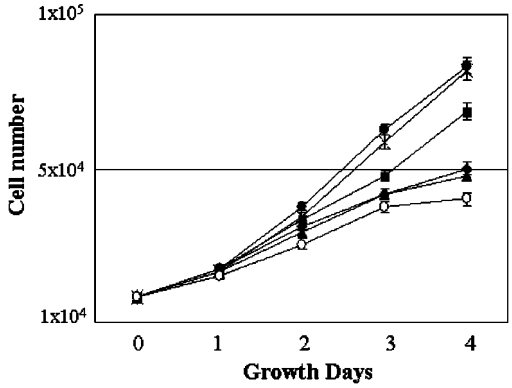

Figure 2. Inhibition of prostate cancer cells proliferation. Cell growth curve of DU145 cells untreated (●), treated with bipyridine (∗), pCurc (■) or complex **1** (▲), LnCaP (◆), and PC3 (○) cells treated with complex **1**. Data are averages of three independent experiments ± standard deviations.

Expression of the glutathione S-transferase, GSTp1 is associated with phase I detoxification of the products of oxidative stress. GSTs play an important role in detoxification by catalyzing the conjugation of electrophilic compounds to glutathione (GSH) such as xenobiotic drugs, toxins, and carcinogens, allowing the drug to be exported from the cell through the GS-X pump.[22] GSTp1 expression has been implicated in the regulation of cell proliferation and apoptosis through direct interaction with the c-Jun NH(2) terminal kinase, (JNK). Hence, GSTp1 protects cells from apoptosis through JNK-mediated mechanisms. Interestingly, in in vitro models, it has been shown that JNK forms a complex with monomeric glutathione transferase class p1−1 (GSTp1−1)[23,24] and this association is inversely correlated with JNK activity. Moreover, recent works demonstrated the role of JNK in curcumin-induced apoptosis.[25,26]

In prostate cancer cells treated with complex **1**, we found a down-regulation of GSTp1 protein after 48 h of exposure and an enhanced phosphorylation of JNK as shown in Figure 4C, indicating a role of this pathway in the apoptosis activated by complex **1** treatment. The densitometric analysis has pointed out that, in all prostate cancer cells, the GSTp1 down-regulation in the case of complex **1** treated cells is two times higher than the one observed in pCurc. Moreover, phosphorylation of JNK is increased in complex **1** treated cells at least 1.5 times when compared to that treated with pCurc.

Overexpression of GSTp1 has been associated with acquired resistance to electrophilic anticancer drugs.[27] The finding that GSTp1 is a modulator of JNK and the relationship between expression of this protein and JNK inhibition suggests that cancer cells prone to overexpress GSTp1 may exhibit high intrinsic JNK inhibitory activity. In this model, tumor cells overexpressing GSTp1 may escape apoptosis, which has been implicated as one of the end-points of JNK activity.[28] Active JNK has been shown to promote ROS detoxification and to

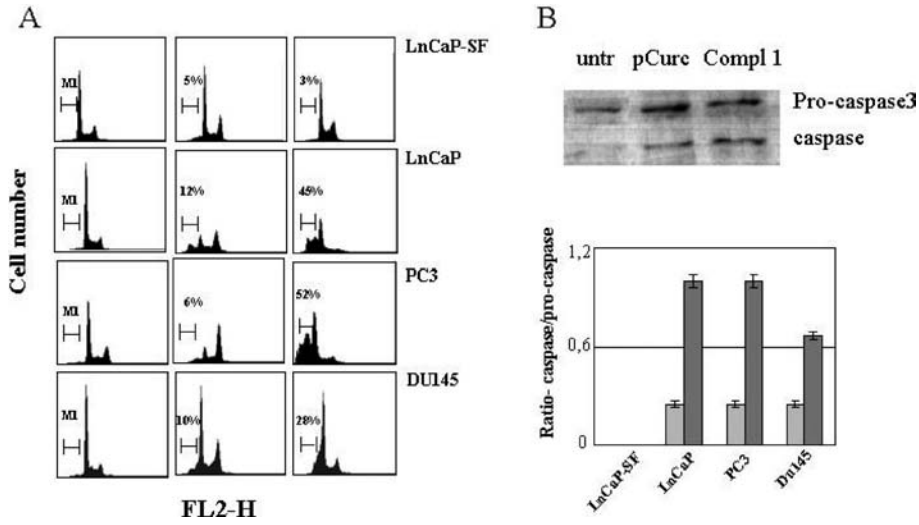

Figure 3. Apoptosis induction in prostate cancer cells by complex **1**. (A) FACS analysis of cell cycle and apoptosis of LnCaP-SF, LnCaP, PC3, and DU145 cells by PI staining after 72 h of exposure to pCurc or complex **1**. (B) Representative caspase-3 cleavage after 48 h of exposure to the compounds evaluated by Western blotting in DU145 cells and densitometric analysis of Western blotting caspase-3 cleavage, evaluated as ratio-caspase/pro-caspase on LnCaP-SF, LnCaP, PC3, and DU145 pCurc (light-gray bars) and complex **1** (medium-gray bars) treated cells. All data are representative of three independent experiments.

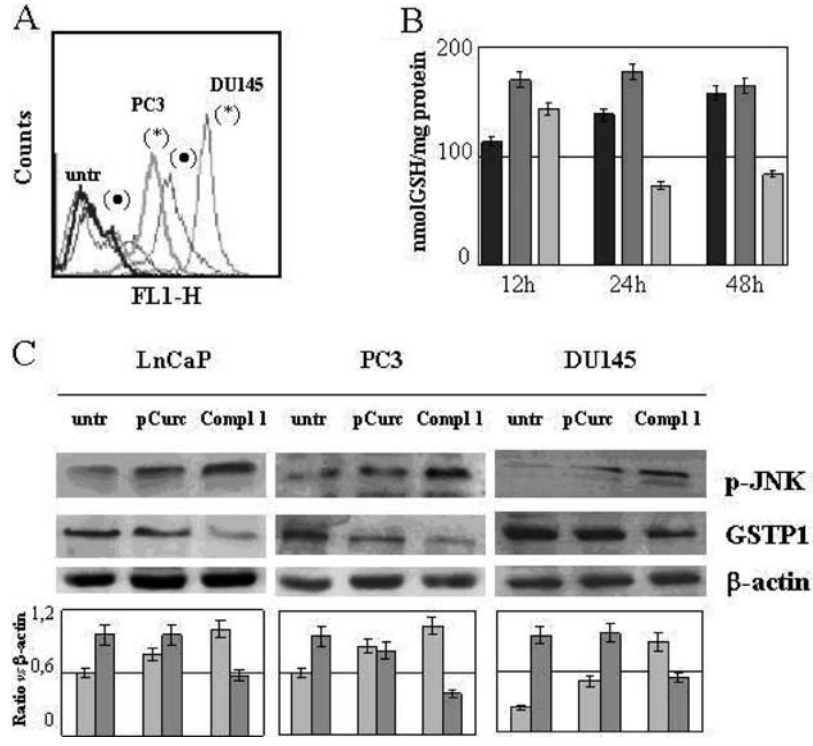

Figure 4. Effect of complex **1** on GSH and GSTp1, evaluation of ROS generation and induction of JNK phosphorylation. (A) FACS analysis of ROS formation in PC3 and DU145 cells after 24 h of treatment with pCurc (*) or complex **1** (●). (B) GSH concentration (nmol/mg of protein) in DU145 treated with pCurc or complex **1** at different time of exposure, untreated cells (dark-gray bars), pCurc treated cells (medium-gray bars), complex 1 treated cells (light-gray bars). Data are reported as SD of three different experiments. (C) Western blotting and relative densitometric analysis (as a ratio to β-actin signal) of GSTp1 (medium-gray bars) protein expression and phosphorylated-JNK (light-gray bars) protein in prostate cancer cells after 48 of exposure to pCurc or complex **1** (data reported are representative of three independent experiments).

confer tolerance to oxidative stress.[29,30] Hence, this kinase may be involved in preventing ROS-derived secondary necrosis in tumor cells, facilitating tumor cell progression.

Concluding, our data indicate that although complex **1** induces less ROS production than pCurc, is able to deplete cells from GSH production to induce a GSTp1 down-regulation and activate JNK, proving its ability in the modulation apoptosis transduction signaling. Thus we believe that complex **1** avoids the prostate cancer acquired resistance to electrophilic anticancer drugs due to the GSTp protein overexpression. In addition, comparing the purified curcumin, the new compound, complex **1** seems to overcome the GSH detoxification because the α,β-unsaturated carbonyl group is hidden by the metal fragment.[10] We can speculate that oxidant properties of complex **1** are a feature of the rapidly ROS elimination by GSH and activation of JNK associated to the down-regulation of GSTp1.

DNA Damage and PARP Activation. Oxidative modification of redox-sensitive factors and intermediate signaling

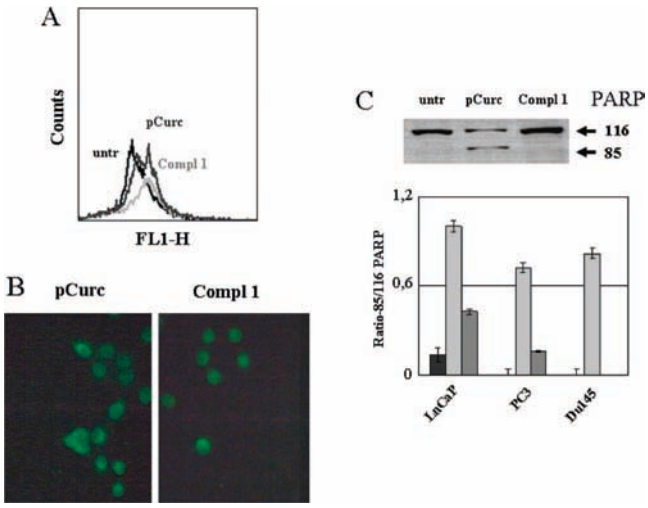

Figure 5. Induction of DNA damage and PARP activation. (A) FACS analysis of DNA damage using Biotrin OxyDNA Assay kit in PC3 and DU145 cells treated with pCurc (∗) or complex **1** (●) for 36 h. (B) Fluorescence images of DU145 cells treated with pCurc (left panel) or complex 1 (right panel), after incubation with the binding protein-FITC conjugate (Biotrin OxyDNA Assay kit). (C) Representative Western blotting analysis of PARP cleavage in DU145 cells after 48 h of exposure to pCurc or complex **1** (upper panel) and densitometric analysis of Western blotting PARP cleavage, evaluated as ratio-85/116 on LnCaP, PC3 and DU145 pCurc (light-gray bars) and complex 1 (medium-gray bars) treated cells. Data are representative of three independent experiments.

molecules (JNK) are involved in ROS-mediated modulation of cell growth and cell survival, characterized by the induction of apoptosis or necrosis.[31] ROS and reactive sulfur species may act concurrently in the damage of biomolecules such as DNA, possibly resulting in the induction of apoptosis or mutagenicity.[32] In fact, ROS can cause single-strand base oxidative modification, single-strand nicks, and DNA double-strand breaks.[33] Among the single-strand base damage identified so far, the guanine-derived modification, 8-*oxo*-2-deoxyguanosine (8-oxo-dG) is the major oxidative lesion.[34,35] The level of 8-oxo-dG in DNA has, therefore, been used consistently as a measure of DNA oxidative damage in previous studies.[34]

In DU145 cells, we found that complex **1** did not affect DNA structure, while pCurc determined DNA damage as proved by the 8-oxo-dG-FACS analysis reported in Figure 5A, and by fluorescent microscopy examination (Figure 5B), after 24 h of exposure. Same data are obtained in PC3 cells. Moreover, pCurc treatment (48 h) induced DNA repair enzyme poly(ADP-ribose) polymerase (PARP) cleavage (Figure 5C) in DU145 and PC3 cells, suggesting that PARP activation appears to contribute to the recovery of prostate cancer cells from DNA damage caused by this agent. Indeed, it is known that PARP activation rescues tumor cells from DNA damage induced by chemotherapy agents. It has been shown that PARP activation may contribute to resistance to conventional chemotherapy agents by facilitating repair of the DNA damage caused by these agents.[36−38] Right now, our data indicate that complex **1** avoids PARP activation inducing apoptosis by JNK phosphorylation, while the DNA-damage induced by pCurc is rescued from PARP activation. The same mechanism of action is observed in all prostate cancer cell lines analyzed.

ΔΨmt Depolarization and Apoptosis-Related Proteins Expression in Complex 1-Treated Cells. JNK activation, normally found occurring in the nucleus, can also be activated in the mitochondria, usually in association with the increased production of reactive oxygen species (ROS). In fact, JNK is known to be activated in response to stress and its activation classically results in the translocation of JNK to the nucleus. However, JNK has also been seen to translocate to the mitochondria in response to stress signals. In most examples, where active JNK is located in the mitochondria, this enzyme colocalizes with and inactivates Bcl-2 or Bcl-XL, facilitating the release of cytochrome c and apoptosis.[39,40]

We evaluated the expression of proteins directly involved in apoptosis via mitochondria as shown in Figure 6A. We found that Bcl-2 protein was down-regulated in complex **1** prostate cancer-treated cells and Bax in the same sample was up-regulated, while pCurc did not affect the expression of both proteins in the cells. Moreover, we may assess that a consequence of Bcl-2 down-regulation and Bax up-regulation in complex **1** treated cells could be a modification of mitochondrial membrane depolarization (ΔΨmt).[41] Figure 6B shows JC1 fluorescence representative dot plots of DU145 cells treated with pCurc and complex **1**. As positive control of JC1 fluorescence, the protonophore CCCP was used. We found that complex **1** was able to induce 38% loss of ΔΨm, two times more than pCurc ΔΨm, in DU145 cells. Moreover, in PC3 cells, we observed a 41% loss of ΔΨm compared to pCurc (15%) and in LnCaP cells ΔΨm loss induced by complex **1** was 12.8%, corresponding to the down-regulation of Bcl-2 protein (densitometric analysis). These data indicate that complex **1** is able to induce apoptosis not only by eliciting its oxidant properties, through JNK activation but also modulating Bcl-2 and Bax expression with induction of mitochondrial membrane depolarization.

Conclusion

The synthesis and characterization of a ionic complex **1** of general formula [(bipy)Pd(pCurc)][CF_3SO_3], containing two different chelating ligands, both biologically active, has been performed. This design strategy aims to determine a synergism around the metal center in order to improve the performances of the single components, namely a bipyridine and the curcumin, affording a new generation of anticancer agent with peculiar oxidant properties. Complex **1** has been tested in vitro toward different human prostate cancer cell lines (LnCaP-SF, LnCaP, PC3, and DU145), and its biological activity has been compared to those of purified curcumin (pCurc). This study indicates clearly that, while pCurc produces a cell growth delay due to the G2 phase arrest in the prostate cancer cells lines analyzed, complex **1** induces cell growth inhibition and apoptosis in hormon-indipendent prostate cancer cells. Interestingly, both complex **1** and pCurc do not elicit an analogous biological effect on hormone-dependent cell line (LnCaP-SF), maybe due to the low proliferation rate of this cell line. Moreover, the ROS production due to the treatment of prostate cancer cells with complex **1** is able to induce JNK phosphorylation with concomitant GSTp1 down-regulation and GSH depletion. Hence, the apoptosis observed in cells treated with complex **1** is mediated by JNK activation and also by mitochondrial membrane depolarization in association with up-regulation of Bax and down-regulation of Bcl2 proteins. On the other hand, the ROS production due to pCurc treatment induces DNA damage with PARP activation, which could cause the cell rescue through G2 arrest and growth delay.

Concluding, the heteroligand mononuclear complex **1** has been found to be significantly more effective than pure curcumin, suggesting that the dual function approach that combines two biological mechanisms in a single molecule significantly improves the biological activity of metal-based

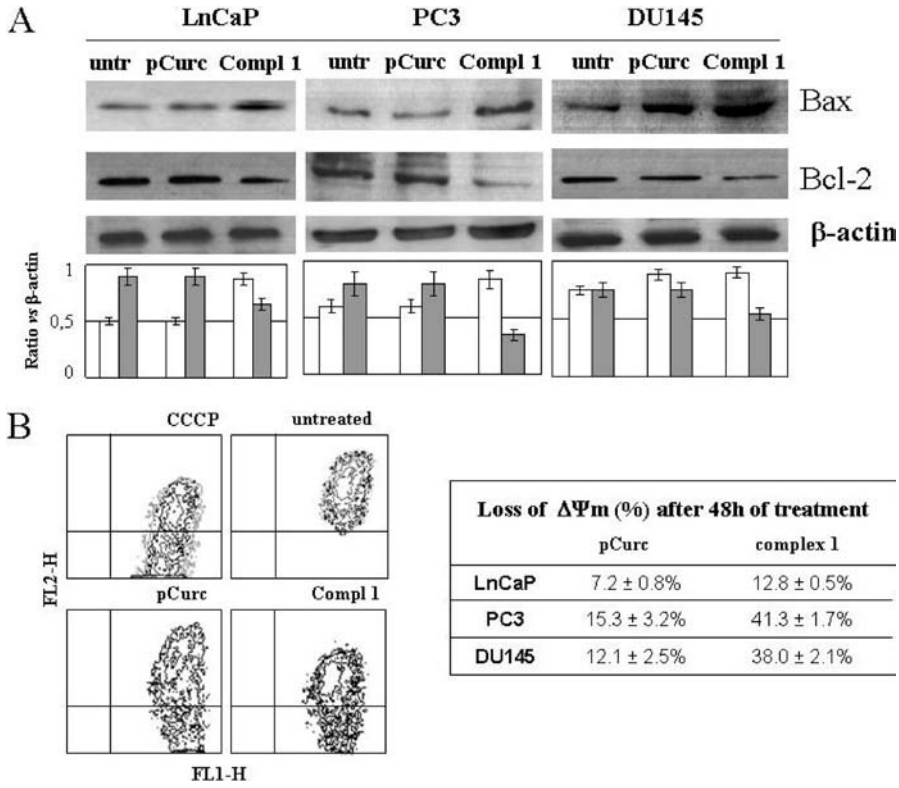

Loss of ΔΨm (%) after 48h of treatment		
	pCurc	complex 1
LnCaP	7.2 ± 0.8%	12.8 ± 0.5%
PC3	15.3 ± 3.2%	41.3 ± 1.7%
DU145	12.1 ± 2.5%	38.0 ± 2.1%

Figure 6. Mitochondrial membrane depolarization induced by complex **1** related with Bcl2 down-regulation and Bax up-regulation. (A) Western blotting and relative densitometric analysis (as a ratio to β-Actin signal) of Bax (white bars) and Bcl-2 (medium-gray bars) protein expression in prostate cancer cells after 72 h of exposure to pCurc or complex 1 (data reported are representative of three independent experiments). (B) Representative experiment of mitochondrial membrane depolarization ($\Delta\Psi$mt) on DU145 cells (FACS analysis) as described in the Experimental Section, CCCP-treated cells were used for compensation (FL-1/FL-2) and loss of $\Delta\Psi$m (%) after 48 h of treatment with pCurc and complex **1** in LnCaP, PC3, and DU145 cells. Data are representative of two independent experiments.

drugs. Moreover, because commercial curcumin suffers of the disadvantage of being relatively poor bioavailable for many different reasons (poor absorption and distribution, rapid metabolism, and excretion[42]), new studies have been recently suggesting how variations in the curcumin structure could somehow improve its bioavailability.[43] In this context, complex **1** could overcome these problems because it represents a further structural modification on the curcumin framework through complexation with palladium(II), leading to a highly stable species and increased biological activity. Furthermore this novel Pd(II) derivative could open new perspective in developing molecules that could bypass GSH/GSTp-related detoxification, which is one of the causes of drug resistance and androgen-independent proliferation in prostate cancer.[44]

Experimental Section

Materials for Synthesis and Measurements. All commercially available starting materials, potassium triflate [$K(CF_3SO_3)$], 4,4′-dinonyl-2,2′-bipyridine (bipy) (all Aldrich Chemical Co.), were used as received without further purification, while the curcumin, purchased from Aldrich, was used after separation into individual components as previously reported.[11] Infrared spectra were recorded on a Spectrum One FT-IR perkin Elmer spectrometer and ^{1}H NMR spectra on a Bruker AVANCE-300 spectrometer, in $CDCl_3$ solution, with TMS (tetramethylsilane) as internal standard. Elemental analyses were performed with a Perkin-Elmer 2400 analyzer. A CARY 50 UV/vis spectrophotometer was used to record absorption spectra of complex on EtOH and 5% EtOH-D-PBS (phosphate buffered saline pH 7.2) solution.

Synthesis of [(bipy)Pd(Pcurc)][CF_3SO_3], 1. Equimolar amount of $Pd(OAc)_2$ was added to a solution of 4,4′-dinonyl-2,2′-bipyridine (0.5 g, 1.22 mmol) in methanol (20 mL). The resulting yellow solution was stirred at room temperature for 20 h. The solution was filtered, and the solvent was removed under vacuum. The remaining residue was extracted and, after crystallization from hexane, the pure yellow solid, of formula [(bipy)$Pd(OAc)_2$] was obtained. Yield: 0.61 g (80%); mp: 181 °C. ^{1}H NMR (300 MHz, $CDCl_3$): δ = 8.07 (d, J (H,H) = 5.82 Hz, 2H, $H_{6,6'}$), 7.97 (s, 2H, $H_{3,3'}$), 7.19 (d, J (H,H) = 5.6 Hz, 2H, $H_{5,5'}$), 2,77 (t, 4H, J (H,H) = 7.2 Hz $CH_2(CH_2)_7CH_3$), 2.12 (s, 6H, $OCOCH_3$), 1.66 (m, 4H, $CH_2(CH_2)_6CH_3$), 1.30 (m, 24H, $(CH_2)_6CH_3$), 0.88 (t, J (H,H) = 6.5 Hz, 6H, CH_3). IR (KBr): 1359 (ν asymmCO_2), 1630 (ν symmCO_2), 2854−2925 (ν C−H).

$K(CF_3SO_3)$ (0.044 g, 0.236 mmol) and pCurc (0.087 g, 0.236 mmol) were added to a solution of this precursor complex [(bipy)$Pd(OAc)_2$] (0.15 g, 0.236 mmol) in methanol (15 mL). The resulting red solution was stirred at room temperature for 20 h. After removal of the solvent under vacuum, the remaining residue was extracted and recrystallized from ether of petroleum to afford the pure complex. Yield: 0.17 g (70%); mp: 210 °C. ^{1}H NMR (300 MHz, $CDCl_3$): δ = 8.17 (d, J (H,H) = 5.8 Hz, 2H, $H_{6,6'}$), 7.71 (s, 2H, $H_{3,3'}$), 7.29 (d, J (H,H) = 5.1 Hz, 2H, $H_{5,5'}$), 7.05 (s, 2H, $H_{g,g'}$), 6.94 (m, 4H, $H_{d,d',e,e'}$), 6.78 (d, J (H,H) = 8.19 Hz, 2H, $H_{f,f'}$), 6.17 (d, J (H,H) = 15.7 Hz, 2H, $H_{c,c'}$), 5.88 (s, 1H, OH), 5.52 (s, 1H, H_b), 3.91 (s, 6H, OCH_3), 2.33 (t, J (H,H) = 7.3 Hz, 4H, $CH_2(CH_2)_7CH_3$), 1.58 (m, 4H, $CH_2(CH_2)_6CH_3$), 1.20 (m, 24H, $(CH_2)_6CH_3$), 0.90 (t, J (H,H) = 6.7 Hz, 6H, CH_3). IR (KBr): 1509 cm^{-1} (ν C−C−C), 1592 (ν C−O curcumin), 1620 (ν C−O), 2855−2927 (ν C−H).

Cytotoxicity and Cell Growth Inhibition. Human prostate cancer cell lines (LnCaP, PC3, and DU145) were grown in RPMI-1640 (Gibco) supplemented with 10% of fetal bovine serum (GIBCO), 5% of L-glutamine (GIBCO) and antibiotics, under standard conditions (37 °C temperature, 5% CO_2 in a humidified atmosphere). All the experiments have been performed at the earlier passage of the cell lines.

To generate prostate cancer cells androgen-dependent (LnCaP-SF), the LnCaP cells were maintained for more than three days in a steroid-free environment with phenol red-free RPMI 1640 medium supplemented with charcoal/dextran-treated FBS to remove the endogenous steroids.

For cytotoxic assays (MTS) and IC_{50} evaluation, cells were plated in 96-well plates (Falcon, CA) in 100 μL of culture medium. For each experiment, pCurc or complex **1** were serially diluted in cell culture medium to the desired concentrations and an equal volume of the diluted solution (100 μL/well) was added to the cells, which were continuously exposed to compounds for 72 h. Each treatment was performed in triplicate in three independent experiments.

Cell viability was determined by the colorimetric 3-(4,5-dimethylthiazol-2-yl)-5-(3-carboxymethoxyphenyl)-2-(4-sulfophenyl)-2*H*-tetrazolium, inner salt (MTS) assay using CellTiter 96 AQueous One solution proliferation assay system (Promega). This assay measures the bioreduction by intracellular dehydrogenases of the tetrazolium compound MTS in the presence of the electron coupling reagent phenazine methosulfate. The plates were incubated 2 h at 37 °C, and then the absorbance at 490 nm was measured using Sirio-S (SEAC, Radim Group), results are expressed as mean ± standard deviation (SD) of the percentage of viable cells at each drug concentration compared to the untreated cells. Then IC_{50} value was calculated by using GraFit32 program. Cell growth inhibition and viability of prostate cancer cells were evaluated following the growth curves by trypan blue exclusion test.

ROS Analysis and Assay of Oxidative DNA Damage. For the ROS content analysis, pCurc and complex **1**-treated adherent cells were first assayed for viability by trypan blue dye exclusion and then incubated with 4 mM dihydroethidium (Molecular Probes, Eugene, OR) for 45 min at 37 °C. After incubation, the cells were analyzed by flow cytometry. ROS production was evaluated 12, 24, and 48 h after the end of pCurc and complex **1** treatment (2 mg/mL for 2 h). As internal ROS control, cells were treated with a solution 15 mM H_2O_2 for 1 h. Untreated and H_2O_2-treated viable cells were analyzed for the ROS production as described above.

A Biotrin OxyDNA assay kit (Biotrin International Ltd., Ireland) was used for the evaluation of oxidative DNA damage. Briefly, after cells were fixed and permeabilized, the FITC labeled protein conjugate was added. The conjugate protein was able to bind the 8-oxoguanine moiety present in the 8-oxoguanosine of oxidized DNA. Hence, by this method, the presence of oxidized DNA was indicated by a green/yellow fluorescence. Using the kit, cells can be analyzed by FACScan or fluorescence microscopy.

Western Blotting. Total cell lysates were obtained resuspending the cells in buffer containing 1% Triton, 0.1% SDS, 2 mM $CaCl_2$, 100 μg/mL phenylmethyl sulfonyl fluoride, and orthovanadate. Protein content was determined using the Protein Assay Kit 2 (Bio-Rad Laboratory, Hercules, CA). Then 30 μg of proteins were electrophoresed in 10% SDS-polyacrylamide gel and then electrotransferred to nitrocellulose membrane (Amersham Biosciences, Piscataway, NJ), which was then blocked overnight with 10 mM Tris-HCl, pH 8.0, 150 mM NaCl, 0.05% Tween-20 (TBS-T) containing 5% nonfat dry milk. The membrane was then incubated with 1 μg/mL of primary antibody in TBS-T [PARP (clone C2−10, BD PharMingen), p-JNK (clone G7, Santa Cruz Biotechnology), GSTp (Calbiochem San Diego, CA), Bax (BD PharMingen), Bcl-2 (clone 124, DakoCytomation), Caspase 3 (Alexis, Switzerland), β-actin (clone Ac-15, Abcam)], and with specific horseradish peroxidase-conjugated secondary antibodies in TBS-T. Protein bands were visualized using a chemioluminescent detection system (Amersham biosciences, Piscataway, NJ). All signals were analyzed densitometrically by using quantified Quantity One (Bio-Rad). The expression of a given protein was expressed as a ratio to β-actin or uncleaved protein, and all data were summarized as the mean and SD.

Determination of Glutathione. Intracellular glutathione was assayed upon formation of *S*-carboxymethyl derivatives of free thiols with iodoacetic acid, followed by the conversion of free amino groups to 2,4-dinitrophenyl derivatives by the reaction with 1-fluoro-2,4-dinitrobenzene as previously described.[45] Data are expressed as nmol of GSH/mg protein.

FACS Analysis of Apoptosis and Mitochondrial Membrane Potential ($\Delta\Psi$mt). For apoptosis analysis, cells were incubated to IC_{50} value of pCurc or complex **1**, and after 48 and 72 h, cells were fixed in ice-cold 75% ethanol and stored at least 1 h at −20 °C. After washing, cells were resuspended in PBS containing 50 U/mL RNase and 50 μg/mL propidium iodide and incubated 1 h in the dark at room temperature. Apoptotic cells were detected by a quantifiable peak in sub-G1 phase corresponding to the red fluorescent light emitted by subdiploid nuclei of cells, and the results were expressed as the percentage of death by apoptosis induced by treatments. Analysis was performed on a FACScan flow cytometer (Becton Dickinson, CA) using CellQuest and ModFit software.

Alterations in the $\Delta\Psi$mt were analyzed by flow cytometry using the $\Delta\Psi$mt-sensitive dye JC1 (5,5′6,6′-tetrachloro-1,1′,3,3′-tetraethylbenzimidazolcarbocyanine iodide; Molecular Probes). Briefly, following treatment, cells were harvested, washed once, and then resuspended in PBS 1×, incubated with 1 μM JC1 at 37 °C for 10 min. Stained cells were then washed once in PBS 1× and analyzed by flow cytometry. A FACScan flow cytometer (Becton Dickinson, Sunnyvale, CA) was used to analyze a minimum of 10000 cells per sample. Data were acquired in list mode and evaluated using a CellQuest software package (Becton Dickinson). Forward and side scatter were used to gate viable population of cells. JC1 monomer (membranebound) emit at 527 nm (FL-1 channel), and "*J*-aggregates" (aqueous phase) emit at 590 nm (FL-2 channel). Protonophore carbonylcyanide *m*-chlorophenylhydrazone (CCCP)-treated cells were used for compensation (FL-1/FL-2). $\Delta\Psi$mt was calculated as a ratio of the fluorescence of *J*-aggregate and monomer forms of JC1.

Acknowledgment. Financial support received from the Ministero dell'Istruzione, dell'Università della Ricerca (MIUR) through the Centro di Eccellenza CEMIF−CAL (CLAB01TYEF) and from Progetto Prosica POR Calabria (misura 316.A.3) grant are gratefully acknowledged.

Supporting Information Available: Elemental analysis for complex **1** and its precursor. This material is available free of charge via the Internet at http://pubs.acs.org.

References

(1) Kellof, J. G. Strategy and planning for chemopreventive drug development: clinical development plans: curcumin. *J. Cell. Biochem.* **1996**, *26S*, 54–71.
(2) Lin, L.; Shi, Q.; Nyarko, A. K.; Bastow, K. F.; Wu, C. C.; Su, C. Y.; Shih, C. C.; Lee, K. H. Antitumor agents. 250. Design and synthesis of new curcumin analogues as potential antiprostate cancer agents. *J. Med. Chem* **2006**, *49*, 3963–3972.
(3) Youssef, K. M.; El-Sherbeny, M. A.; El-Shafie, F. S.; Farag, H. A.; Al-deeb, O. A.; Awadalla, S. A. A. Synthesis of curcumin analogues as potential antioxidant, cancer chemopreventive agents. *Arch. Pharm.* **2004**, *337*, 42–54.
(4) Odot, J.; Albert, P.; Carlier, A.; Tarpin, M.; Devy, J.; Madoulet, C. In vitro and in vivo anti-tumoral effect of curcumin against melanoma cells. *Int. J. Cancer* **2004**, *111*, 381–387.
(5) Mukhopadhyay, A.; Bueso-Ramos, C.; Chatterjee, D.; Pantazis, P.; Aggarwal, B. B. Curcumin downregulates cell survival mechanisms in human prostate cancer cell lines. *Oncogene* **2001**, *20*, 7597–7609.
(6) Cao, J.; Liu, Y.; Jia, L.; Zhou, H. M.; Kong, Y.; Yang, G.; Jiang, L. P.; Li, Q. J.; Zhong, L. F. Curcumin induces apoptosis through mitochondrial hyperpolarization and mtDNA damage in human hepatoma G2 cells. *Free Radical Biol. Med.* **2007**, *43*, 968–975.
(7) Nishinaka, T.; Ichijo, Y.; Ito, M.; Kimura, M.; Katsuyama, M.; Iwata, K.; Miura, T.; Terada, T.; Yabe-Nishimura, C. Curcumin activates human glutathione S-transferase P1 expression through antioxidant response element. *Toxicol. Lett.* **2007**, *170*, 238–247.
(8) Fujisawa, S.; Atsumi, T.; Murakami, Y.; Kadoma, Y. Dimerization, ROS formation, and biological activity of *o*-methoxyphenols. *Arch. Immunol. Ther. Exp.* **2005**, *53*, 28–38.
(9) Atsumi, T.; Fujisawa, S.; Tonosaki, K. Relationship between intercellular ROS production and membrane mobility in curcumin- and tetrahydroxycurcumin-treated human gingival fibroblasts and

human submandibular gland carcinoma cells. *Oral. Dis.* **2005**, *11*, 236–242.
(10) Awasthi, S.; Pandya, U.; Singhal, S. S.; Lin, J. T.; Thiviyanathan, V., Jr.; Awasthi, Y. C.; Ansari, G. A. Curcumin-glutathione interactions and the role of human glutathione S-transferase P1−1. *Chem.−Biol. Interact.* **2000**, *128*, 19–38.
(11) Pucci, D.; Bloise, R.; Bellusci, A.; Bernardini, S.; Ghedini, M.; Pirillo, S.; Valentini, A.; Crispini, A. Curcumin and cyclopalladated complexes: a recipe for bifunctional biomaterials. *J. Inorg. Biochem.* **2007**, *101*, 1013–1022.
(12) Bernabé-Pineda, M.; Ramìrez-Silva, M. T.; Romero-Romo, M.; Gonzalez-Vergara, E.; Rojas-Hernandez, A. Determination of acidity constants of curcumin in aqueous solution and apparent rate constant of its decomposition. *Spectrochim. Acta, Part A* **2004**, *60*, 1091–1097.
(13) Ansari, M. J.; Ahmad, S.; Kohli, K.; Ali, J.; Khar, R. K. Stability-indicating HPTLC determination of curcumin in bulk drug and pharmaceutical formulations. *Pharmaceut. Biomed. Anal.* **2005**, *39*, 132–138.
(14) Atsumi, T.; Tonosaki, K.; Fujisawa, S. Induction of early apoptosis and ROS-generation activity in human gingival fibroblasts (HGF) and human submandibular gland carcinoma (HSG) cells treated with curcumin. *Arch. Oral Biol.* **2006**, *51*, 913–921.
(15) Hail, N., Jr. Mitochondrial reactive oxygen species affect sensitivity to curcumin-induced apoptosis. *Free Radical Biol. Med.* **2008**, *44*, 1382–1393.
(16) Nogaki, A.; Satoh, K.; Iwasaka, K.; Takano, H.; Takahama, M.; Ida, Y.; Sakagami, H. Radical intensity and cytotoxic activity of curcumin and gallic acid. *Anticancer Res.* **1998**, *18*, 3487–3491.
(17) Ogata, M.; Hoshi, M.; Urano, S.; Endo, T. Antioxidant activity of eugenol and related monomeric and dimeric compounds. *Chem. Pharm. Bull.* **2000**, *48*, 1467–1469.
(18) Ogiwara, T.; Satoh, K.; Kadoma, Y.; Murakami, Y.; Unten, S.; Atsumi, T.; Sakagami, H.; Fujisawa, S. Radical scavenging activity and cytotoxicity of ferulic acid. *Anticancer Res.* **2002**, *22*, 2711–2718.
(19) Zheng, S.; Yumei, F.; Chen, A. De novo synthesis of glutathione is a prerequisite for curcumin to inhibit hepatic stellate cell (HSC) activation. *Free Radical Biol. Med.* **2007**, *43*, 444–453.
(20) Scott, D. W.; Loo, G. Curcumin-Induced GADD153 Upregulation: Modulation by Glutathione. *J. Cell. Biochem.* **2007**, *101*, 307–320.
(21) Ercal, N.; Gurer-Orhan, H. N.; Aykin-Burns, N. Toxic metals and oxidative stress part I: mechanisms involved in metal-induced oxidative damage. *Curr. Top. Med. Chem.* **2001**, *1*, 529–539.
(22) Schmid, M.; Zimmermann, S.; Krug, H. F.; Sures, B. Influence of platinum, palladium and rhodium as compared with cadmium, nickel and chromium on cell viability and oxidative stress in human bronchial epithelial cells. *Environ. Int.* **2007**, *33*, 385–390.
(23) Duvoix, A.; Morceau, F.; Delhalle, S.; Schmitz, M.; Schnekenburger, M.; Galteau, M. M.; Dicato, M.; Diederich, M. Induction of apoptosis by curcumin: mediation by glutathione S-transferase P1−1 inhibition. *Biochem. Pharmacol.* **2003**, *66*, 1475–1483.
(24) Valentini, A.; Gravina, P.; Bernardini, S.; Federici, G. Role of glutathione S- transferase in the cellular antioxidant defence. In *Enzymes and Cellular Fight against Oxidation*; Transworld Research Network Ed: Kerala, India, 2008, Chapter 5.
(25) Adler, V.; Yin, Z.; Fuchs, S. Y.; Benezra, M.; Rosario, L.; Tew, K. D.; Pincus, M. R.; Sardana, M.; Henderson, C. J.; Wolf, C. R.; Davis, R. J.; Ronai, Z. Regulation of JNK signalling by GSTp. *EMBO J.* **1999**, *18*, 1321–1334.
(26) Kamath, R.; Jiang, Z.; Sun, G.; Yalowich, J. C.; Baskaran, R. Abl kinase regulates curcumin-induced cell death through activation of JNK. *Mol. Pharmacol.* **2007**, *71*, 61–72.
(27) Nakagawa, K.; Saijo, N.; Tsuchida, S.; Sakai, M.; Tsunokawa, Y.; Yokota, J.; Muramatsu, M.; Sato, K.; Terada, M.; Tew, K. D. Glutathione-S-transferase pi as a determinant of drug resistance in transfectant cell lines. *J. Biol. Chem.* **1990**, *265*, 4296–301.
(28) Yong-sook, K.; Deok-young, J.; Kee-young, L. Involvement of ROS and JNK1 in selenite-induced apoptosis in Chang liver cells. *Exp. Mol. Med.* **2004**, *36*, 157–164.
(29) Venugopal, R.; Jaiswal, A. K. Nrf2 and Nrf1 in association with Jun proteins regulate antioxidant response element-mediated expression and coordinated induction of genes encoding detoxifying enzymes. *Oncogene* **1998**, *17*, 3145–5630.
(30) Wang, M. C.; Bohmann, D.; Jasper, H. JNK signaling confers tolerance to oxidative stress and extends lifespan in *Drosophila*. *Dev. Cell* **2003**, *5*, 811–816.
(31) Fujisawa, S.; Atsumi, T.; Murakami, Y.; Kadoma, Y. Dimerization, ROS formation, and biological activity of *o*-methoxyphenols. *Arch. Immunol. Ther. Exp.* **2005**, *53*, 28–38.
(32) Wiseman, A. Dietary alkyl thiol free radicals (RSS) can be as toxic as reactive oxygen species (ROS). *Med. Hypotheses* **2004**, *63*, 667–670.
(33) Chen, J. H.; Hales, C. N.; Ozanne, S. E. DNA damage, cellular senescence and organismal ageing: causal or correlative. *Nucleic Acids Res.* **2007**, *35*, 7417–7428.
(34) Cooke, M. S.; Evans, M. D.; Dizdaroglu, M.; Lunec, J. Oxidative DNA damage: mechanisms, mutation, and disease. *FASEB J.* **2003**, *17*, 1195–1214.
(35) Evans, M. D.; Dizdaroglu, M.; Cooke, M. S. Oxidative DNA damage and disease: induction, repair and significance. *Mutat. Res.* **2004**, *67*, 1–61.
(36) Bouchard, V. J.; Rouleau, M.; Poirier, G. G. PARP-1, a determinant of cell survival in response to DNA damage. *Exp. Hematol.* **2003**, *31*, 446–454.
(37) Madhusudan, S.; Middleton, M. R. The emerging role of DNA repair proteins as predictive, prognostic and therapeutic targets in cancer. *Cancer. Treat. Rev.* **2005**, *31*, 603–617.
(38) Tentori, L.; Graziani, G. Chemopotentiation by PARP inhibitors in cancer therapy. *Pharmacol. Res.* **2005**, *52*, 25–33.
(39) Ito, Y.; Mishra, N. C.; Yoshida, K.; Kharbanda, S.; Saxena, S.; Kufe, D. Mitochondrial targeting of JNK/SAPK in the phorbol ester response of myeloid leukemia cells. *Cell. Death Differ.* **2001**, *8*, 794–800.
(40) Kharbanda, S.; Saxena, S.; Yoshida, K.; Pandey, P.; Kaneki, M.; Wang, Q.; Cheng, K.; Chen, Y. N.; Campbell, A.; Sudha, T.; Yuan, Z. M.; Narula, J.; Weichselbaum, R.; Nalin, C.; Kufe, D. Translocation of SAPK/JNK to mitochondria and interaction with Bcl-x(L) in response to DNA damage. *J. Biol. Chem.* **2000**, *275*, 322–327.
(41) Shoshan-Bramatz, V.; Israelson, A.; Brdiczka, D.; Sheu, S. S. The voltage-dependent anion channel (VDAC): function in intracellular signalling, cell life and cell death. *Curr. Pharm. Des.* **2006**, *12*, 2249–2270.
(42) Anand, P.; Kunnumakkara, A. B.; Newman, R. A.; Aggarwal, B. B. Bioavailability of Curcumin: Problems and Promises. *Mol. Pharmaceutics* **2007**, *4*, 807–818.
(43) Liu, A.; Lou, H.; Zhao, L.; Fan, P. Validated LC/MS/MS assay for curcumin and tetrahydrocurcumin in rat plasma and application to pharmacokinetic study of phospholipid complex of curcumin. *J. Pharm. Biomed. Anal.* **2006**, *40*, 720–727.
(44) Hokaiwado, N.; Takeshita, F.; Naiki-Ito, A.; Asamoto, M.; Ochiya, T.; Shirai, T. Glutathione S-transferase pi mediates proliferation of androgen-independent prostate cancer cells. *Carcinogenesis* **2008**, *29*, 1134–8.
(45) Ciriolo, M. R.; Aquilano, K.; De Martino, A.; Carrì, M. T.; Rotilio, G. Differential role of superoxide and glutathione in *S*-nitrosoglutathione-mediated apoptosis: a rationale for mild forms of familial amyotrophic lateral sclerosis associated with less active Cu, Zn superoxide dismutase mutants. *J. Neurochem.* **2001**, *77*, 1433–1443.

JM801276A